6. Functional Neuroanatomy of Heading Perception in Humans

Lucia M. Vaina[1,2] and Sergei Soloviev[1]

[1] Brain and Vision Research Laboratory, Department of Biomedical Engineering
Boston University, Boston, MA, USA

[2] Department of Neurology
Harvard Medical School, Boston, MA, USA

1 INTRODUCTION

As we move through the environment, the pattern of visual motion on the retina provides rich information about our passage through the scene. There is an abundant physiological and psychophysical evidence that this information, termed "optic flow" (Gibson, 1950), is an essential component of navigation in the three-dimensional space, since it is critical for encoding self-motion, for the perception of object movement and for controlling posture and locomotion. Psychophysical experiments have demonstrated that human observers can recover with high accuracy the direction of heading from optic flow patterns, even in the absence of actual self-motion (Warren, 1998, 1999). Electrophysiological studies on the 'motion system' in the dorsal extrastriate cortex in monkeys have identified cortical areas that might provide the neural substrate for the analysis of optic flow patterns and for the direction of self-motion (heading). In particular, the dorsal medial division of the macaque middle superior temporal area (dMST) has been proposed to be specialized for the analysis of complex optic flow information (Albright, 1993; Albright & Stoner, 1995; Andersen, 1997; Andersen et al., 2000; Wurtz & Duffy, 1992) and recent studies (Britten & Van Wezel, 1998, 2002) have shown that neurons in this area are also involved in recovering self-motion direction from optic flow cues.

Particularly relevant for this chapter are the results from recent research on electrical stimulation of MST neurons in monkeys trained to indicate the side of the display containing the focus of optic flow expansion (Britten & Van Wezel, 1998, 2002). These studies reported that the monkey's indication

of heading location was influenced by the activity of the MST neurons altered by electrical stimulation and the shift of responses was in the direction expected from the visual stimulus and the preference of the activated neurons — thus when electrically stimulated neurons had preference for left heading, the monkey's response was also biased toward left heading. This is the first strong evidence for the fact that MST neurons directly contribute to the computations underlying the direction of self-motion (heading) from optic flow. Is MST the only cortical area significantly involved in computing heading? A number of physiological studies showed that several other motion responsive cortical areas, especially parietal area 7a may provide additional neural substrate for mechanisms involved in optic flow computation ((Siegel & Read, 1997) and see Chapter 1, for a review). Does each of these areas compute optic flow and perhaps heading, or do they operate in concert in a network of neural mechanisms to mediate different aspects of these computations? In this chapter we partially address this question by examining some of the recent functional neuroimaging literature on optic flow and heading direction discrimination in healthy human subjects. However, as pointed out by Wurtz (1998), just the perceptual investigation will not give us the full answer since in the psychophysical tasks observers are asked to indicate to which side of a reference mark they are heading, and it is the experimenter's inference that the responses reflect a judgment of heading. However, this is the best approximation of the problem we now have on our hands, before quantitative studies of heading estimation in subjects navigating in the real everyday environment will emerge with some consistency.

2 CORTICAL AREAS RESPONSIVE TO OPTIC FLOW REVEALED BY FMRI IN HUMANS

In humans, functional neuroimaging studies (PET and fMRI) have repeatedly reported that many regions in the human brain respond selectively to moving stimuli (Braddick et al., 2001; Dupont et al., 1994; Grezes et al., 2001; Grossman et al., 2000; Grossman & Blake, 2002, Servos et al., 2002; Sunaert, 2001; Sunaert et al., 1999; Tootell et al., 1997; Vaina et al., 2001). Most of the studies published thus far have investigated the anatomical areas of activation and the extent to which cortical activation, as measured by stimulus-evoked changes in blood flow and tissue oxygenation, are characteristic of specific motion tasks.

A large number of studies have concentrated on a region in the ascending limb of the inferior temporal sulcus referred to as hMT+ because it functionally represents the human homologue of the macaque areas MT and MST (Beauchamp & DeYoe, 1996; Braddick et al., 2001; Cheng et al., 1995;

Dumoulin et al., 2003; Dupont et al., 1994, McKeefry et al., 1997; Reppas et al., 1997; Tootell et al., 1993, 1995a, 1995b, 1998; Watson et al., 1993; Zeki et al., 1991). In particular, when Tootell et al. (1995b) mapped BOLD (blood oxygenation level-dependent) responses in the striate and extrastriate visual areas to motion stimuli portraying radial gratings, they found that the hMT+ strongly responded to low contrast stimuli (it saturated already at 4% contrast). Orban and collaborators conducted several combined functional neuroimaging (both PET and fMRI) and psychophysical studies of direction and speed discrimination of frontoplanar random dot motions (Dupont et al., 1994, 1997; Orban, 2001; Sunaert et al., 1999, 2000; Van Oostende et al., 1997), which strengthens the evidence that several areas other than hMT+ are involved in motion processing.

The posterior part of area hMT+ is bound by area V3a, which is also quite sensitive to motion (Tootell et al., 1997). An area anterior to V3a has been designated as the kinetic occipital (KO) area, to reflect sensitivity to the form of structured kinetic stimuli (Dupont et al., 1997; Van Oostende et al., 1997). Area KO responds strongly to motion defined borders in complex motion displays. This area, referred to as V3b by Smith and collaborators (Smith et al., 1998), has been shown to also respond to certain types of second order motion**.**

Recently, several fMRI studies aimed to further subdivide the area hMT+ into two distinct regions suggested as corresponding to the macaque areas MT and MST (Dukelow et al., 2001; Huk et al. 2002; Morrone et al., 2000). In particular, the Huk et al. (2002) study cleverly exploits the physiological evidence from the macaque for a distinguishable retinotopic map in MT and a much coarser retinotopic organization in MST, together with the larger extension into the ipsilateral hemifield of the receptive fields of MST neurons compared to those in MT. Thus, using stimuli specifically devised for assessing retinotopic organization and receptive field size within hMT+, they found two distinct but adjacent regions of activity: one, suggested to be the human homologue of the macaque MT, exhibited retinotopic organization and smaller receptive fields, and the other, corresponding to area MST in the macaque, did not show clear retinotopy but responded to peripheral ipsilateral stimulation consistent with large receptive sizes of its neurons.

3 FUNCTIONAL NEUROIMAGING OF OPTIC FLOW AND OF DIRECTION OF HEADING JUDGMENT

A PET study (de Jong et al., 1994) of the cortical areas responsive to optic flow stimuli simulating forward motion in depth over a flat horizontal surface found bilateral foci of activity in the fusiform and temporal gyri, the right

dorsal cuneus (area V3), and the latero-posterior cuneus (or superior parietal lobe). No significant activity was found in hMT+. The optic flow field in this study consisted of small bright dots on a dark background (viewed binocularly) and comparisons were made between displays with 100% coherent radial expansion motion from a virtual horizon and 0% coherent motion in which all the dots moved in random directions. In a follow up study (Howard et al., 1996), the stimulus was modified to activate both the inferior and superior visual field during fMRI scanning. Significant activation was found in both the dorsal and ventral V3, within the area hMT+ and a region within the superior temporal gyrus (STG), hypothesized by these authors as the probable human equivalent of the macaque superior polysensory area (STP) known to respond to optic flow stimuli (Siegel, 1998; Siegel & Read, 1997).

Using a block design paradigm alternating static dots with random dot kinematograms portraying optic flow, Greenlee (2000) found clusters of activation in the striate (V1) and extrastriate (V2, V3/V3a) cortices, in ventral area V3, in areas KO/V3b and in the hMT+. This interesting study also demonstrated that the hMT+ activation did not vary significantly with the type of optic flow (e.g., rotation or radial). However, area KO/V3b appeared to respond selectively to the disparity gradient present in the optic flow field stimulus In particular, within KO/V3b the disparity effect was measurable in the rotation condition and somewhat less in the expansion condition. Rutchsmann and colleagues (Rutschmann et al., 2000) investigated BOLD responses to optic flow in a paradigm comparing either monoptic or dichoptic presentations of either expansion or expanding-spiral motions with a random-walk stimulus. In the monoptic presentation subjects viewed the optic flow binocularly in plane, with both eyes viewing the same stimulus. In the dichoptic presentation the stimuli were presented with stereo depth, using speed gradients combined with varying amounts of disparity. In a block design experimental paradigm, alternating fixation with one type of optic flow, significant responses to all types of stimuli were found in Brodmann areas (BA) 17, 18, 19 and 37. However, selective response to the direction components of the flow (expansion > spiral > rotation) were found only in the middle portion of area 19, labeled 19m and postulated as equivalent to the functionally defined area KO/V3b (Dupont et al., 1997; Smith et al., 1998; Van Oostende et al., 1997). This provides further support for the involvement of areas KO/V3b in the processing of optic flow. However, there was no stimulus selective response in area hMT+, except under the dichoptic viewing conditions (in the presence of binocular disparity). Furthermore, the dichoptic stimuli also consistently elicited a small increase in response (percent signal increase) in BA 19m (KO/V3b) and BA 19d (putative V3a) which was coupled with the directional component of the flow, possibly representing a

correlate of the additional processing associated with the neural analysis of optic flow in the 3-D conditions (Rutschmann et al., 2000).

These and other studies not discussed here compared moving dots with static stimuli. However, as pointed out by Braddick and collaborators (Braddick et al., 2001) by doing this, cortical areas specifically activated by direction of motion cannot be distinguished from areas activated by temporal frequency (flicker). To address specifically the cortical substrate of motion coherence (direction discrimination) these authors used a block design stimulus paradigm consisting of a uniform moving field of random dots alternating with dynamic noise dots, but keeping throughout the same temporal and spatial frequencies. The results of this study reveal that in the occipital lobe, V1 was not specifically activated by coherent motion, but strong activation was seen in several extrastriate areas, among which most prominently in the areas hMT+, V3a and V3. The unexpected outcome of this study is the strong response to coherent motion in area V3, suggesting that the ventral occipital region is also sensitive to this type of motion. In addition, this study is somewhat at odds with the findings of McKeefery and colleagues (McKeefry et al., 1997) who reported that hMT+ was more strongly activated by incoherent than by coherent motion. One possible explanation for this discrepancy might be that in this latter study (McKeefry et al., 1997) the stimuli had very low dot density, which prevented summation within the receptive field, and thus the directional activation could not predominate in hMT+. Sensitivity to motion coherence, assessed as the increased stimulus-related blood flow, was also reported in the intraparietal sulcus (IPS) and in the superior temporal sulcus (STS).

In a recent PET imaging study Beer and colleagues (Beer et al., 2002) stimulated different types of observer's continuous movements in depth using a very large visual display in order to identify brain areas selective to these movements. They concluded that in order to detect direction of heading and analyze its parameters the brain engages a network of widely distributed regions, particularly KO and several additional sites in the temporal, temporoparietal and occipital areas. Similar to studies discussed above, these authors also found that hMT+ was selectively activated by incoherent motion, but was not selective for the continuous coherent, wide-field motion simulating self-motion.

Peuskens and colleagues (Peuskens et al., 2001) used PET and fMRI to determine the cerebral activation pattern elicited when subjects performed an active task of heading direction discrimination when viewing a ground plane of optic flow. In the PET study the main effect of heading in the occipital and occipital-temporal cortices was a strong activation in the cuneus, with the local maxima in the presumed areas V2 and V3a, and in an area located posterior to the reported location of the hMT+ (Talairach coordinates –44, -80, 4; z-value; z = 7.2 and 40, -82, 4; z = 5.3), (Talairach & Tournoux, 1988).

More anterior, bilateral activation was noted in the superior parietal lobule, in a region located dorsally in the intraparietal sulcus corresponding to the areas DIPSM/DIPSL (medial and dorsal intraparietal sulcus regions), (Sunaert et al., 1999). In a subsequent fMRI study these authors used a passive viewing task for hMT+ localization, in addition to the heading discrimination task. Comparison in the Talairach space of the areas activated by these two tasks revealed that hMT+ was significantly involved in heading discrimination. Further significant activation was also documented in several posterior frontal regions, both in the dorsal and ventral premotor areas, suggesting the linking of heading information to motor plans.

D'Avossa and colleagues (D'Avossa et al., 1998) interested in the spatial coding of heading representation, investigated whether different values of a relevant parameter were represented in different cortical regions. Their approach is quite interesting as it directly addresses the concept of neural maps that have been shown to contain specific representations within different regions of cortex (Knudsen et al., 1987). They used fMRI to determine whether homologous areas of each hemisphere encode heading direction towards the opposite side of the space and to map the azimuthal and elevational components of heading (D'Avossa & Kersten, 1996). The stimulus consisted of random dot kinematograms portraying optic flow which simulated heading toward a 3-D cloud of stationary dots either in the gaze direction or in an eccentric direction (i.e. 3 deg above, below, right or left of the fixation point). In each block of trials optic flow simulating heading straight ahead was paired with optic flow simulating one of the eccentric headings. In accord with previously discussed studies, the cerebral activations during the perception of optic flow simulating self-motion in an eccentric direction activated regions in the occipital and parietal lobes presumably corresponding to the areas V3 and 7a. The lateralization of activity in these areas co-varied with the direction of heading, consistent with a map of heading in either or both of these areas. The anterior regions showed a right hemisphere lateralization irrespective of direction, which may be explained by a possible involvement of attentional mechanisms. Further data analysis of activations points to the involvement in the left hemisphere of the cuneus and the superior parietal lobule, and the cuneus and the medial occipital gyrus bilaterally.

Similar to the results reported by de Jong and colleagues (de Jong et al., 1994), there were no significant activations in the hMT+ to any of the heading stimuli. However, unlike in de Jong's study, here the heading stimuli did not elicit any activation in the ventral occipital-temporal areas. Wunderlich and collaborators (Wunderlich et al., 2002) used fMRI to investigate the neural substrate of perception of objects that appear to move in depth (toward or away from the observer). Such stimuli were alternated in a block design paradigm with a static random dots field. The major question in this study was

whether brain activation elicited by the perception of motion towards the observer is different from activity resulted from motion away from the observer. They found that regions in the lateral inferior occipital cortex bilaterally and the right lateral superior occipital cortex were quite specifically implicated in processing motion toward the observer. The activated region in the superior lateral occipital cortex corresponded to the cortical area KO. The area hMT+ was not differentially activated by dots moving towards the observer.

Different studies used different stimuli parameters and consequently found somewhat different areas of activity. Surprisingly, there was no agreement on the specific sensitivity of hMT+ to the various heading stimuli. The detailed study of Peuskens and collaborators conjectured that if the activation pattern in DIPSM/L can be considered suggestive for this area's central role in heading perception, these parietal regions may correspond, functionally, to the macaque area 7a, which is believed to be the apex of the motion pathway. Neurophysiological studies of Siegel and colleagues (Chapter 1, for a review) suggest that area 7a might be involved in the extrapersonal representation of space and the representation of self-motion, or direction of heading and of object motion. D'Avossa and colleagues (D'Avossa et al., 1998) reported activity in the probable homologue of 7a for rightward and leftward heading, but it is puzzling that no activation was found in the parietal lobes for upward heading.

To further determine the neuro-anatomical substrate of heading perception in humans, here we compare results from fMRI and behavioral studies in three related heading tasks. In the first two, *Heading RDK* and *Heading RDK Objects*, the stimulus consisted of a dynamic random dot patterns simulating heading towards a stationary 3-D cloud of dots towards which the observer moved on a straight path. The *Heading RDK Objects* contained four square objects defined by random dots translating in plane and all crossing the focus of expansion. In the third task, *Heading Landmarks*, the stimulus portrayed a large room populated with different static objects that served as landmarks. In particular, we were interested to determine whether cortical activation in three heading tasks was strongly sensitive to different image cues or to the task itself. Our focus was on comparing the brain regions activated by each of the tasks and on the correlation of behavioral results with activation (BOLD signal percent change) in particular regions of interests (ROIs) identified in the basic fMRI data analysis.

3.1 Subjects and Procedures

Eight naïve, healthy subjects with normal vision (ranging in age between 22-35 years; 4 women) were paid to participate in the study of visual heading. All subjects participated in the psychophysical and the fMRI studies of the tasks described above. The entire study was approved by the ethics committees at the Boston University and the NMR Center at Massachusetts General Hospital and all subjects gave informed consent. Displays were generated by a Power Macintosh G4 and for psychophysics were presented on the Macintosh screen. During fMRI scanning, visual stimuli were rear-projected onto an acrylic screen (DaTex, Da-Lite Corp.) providing an activated visual field up to 40×25 degrees. Stimuli were projected onto the screen by a Sharp 2000 color LCD projector, through a collimating lens (Buhl Optical). Details on the fMRI data acquisition are given in the next section.

Two-three days prior to the fMRI study each subject first underwent a practice session until they felt comfortable with all the tasks (usually 10-15 repetition trials) and then additional thresholds were obtained on each experimental condition from each subject. Feedback was given only during the practice trials. Subjects were instructed to maintain fixation throughout each trial, but the examiner controlled fixation only informally. During the psychophysical testing the room was completely dark except for the display. To obtain estimates of the threshold at which subjects can judge their heading accurately, the angle between the heading and the target line was varied according to an adaptive staircase procedure. A button press on a keypad indicated the response. For the psychophysical tasks, threshold was calculated as the average of the last six reversal values, during which stimulus presentation followed a classical staircase (one error - one step up, three correct response - one step down). The variable in all three tasks was the heading angle defined as the visual angle between the actual heading and the probe. Subjects completed 5-8 repeats of the staircase procedure, until their performance appeared to asymptote three times in a row. A final threshold was calculated for each subject as the mean of the three consecutive similar thresholds. In Figure 1 (d), for each heading task we report the mean of the final thresholds from all subjects.

3.2 The Heading Stimuli

3.2.1 Heading Perception in Random Dot Kinematograms

The first experiment tests the ability of naive observers to judge heading from motion fields that simulate pure translation of the observer in two conditions: (a) the stimulus portrays only the observer's motion toward the stationary scene. The focus of expansion is visible throughout a trail; (b) the scene contains four additional translating objects that cross the observer's path in each trial (and hence the FOE was not visible at all times).

(a) Subjects viewed binocularly optic flow patterns, centered at the fovea, simulating self-motion relative to a 3D cloud of stationary dots. The stimulus consisted of a dynamic random dot field displayed in a square aperture subtending 35.5 deg^2 at 30° viewing distance**.** Dots were randomly generated from the super volume including the visible part at the beginning to obtain constant dot density projection of the environment on the screen. Dot size was 6 $arcmin^2$ and dot density (2 $dots/deg^2$) was algorithmically kept constant. The simulated observer speed was 200 cm/sec, which corresponds to a fast walk of 4.2 miles/hour, or 7.2 km/hour. The direction varied with uniform probability between extreme values of 2.5° and 12° to the left and right of the center of the display.

(b) In this condition we tested how observers' heading judgments were affected by the presence of moving objects. Previous precise psychophysical studies of Royden and Hildreth (1996) and Warren and Saunders (1995) reported that in the presence of a single moving object that crossed the observer's path, there was a small directional bias in the heading judgments. Our focus was on characterizing and comparing the neuroanatomical substrates of these two test conditions, simple straight trajectory heading and heading in the presence of several moving objects crossing the focus of expansion (FOE).

Superimposed on the display described above there were four small objects defined as dynamic occluding planes defined by the difference in speed and direction from the heading pattern defined above. The objects had diameters ranging between 1.75°- 4°, and a constant dot density of 2 $dots/deg^2$. The density of the entire display was held constant at 2 $dots/deg^2$. The dots within the illusory borders of the objects translated relative to the observer within the XY plane at a constant speed of 100 cm/sec at the viewing distance of 30 cm. The motion of the objects was independent relative to the observers' simulated motion. The objects kept a constant linear planar trajectory (two diagonal in opposite directions, one upward and the other downward) and each object intersected once and occluded temporarily the

focus of expansion. Throughout the test the starting positions and direction motions of the objects were kept constant while the observer heading direction was varied from trial to trial by the staircase procedure.

In both experimental conditions, (a) and (b), observers were instructed to fixate on a central fixation mark. They watched a motion sequence for 440 msec at the end of which a vertical white probe was displayed on a newly generated static frame of random dots with the same image characteristics as in the RDK (except motion) at a given horizontal angle from the true heading (FOE). The observers' task was to judge whether it appeared that they were heading to the left or right of the vertical probe line. A button press on a keypad indicated the observer's responses. Prior to task (b), subjects were told that moving objects would be present and they were asked to ignore them as much as possible and to base their response to their perceived movement toward the 3D cloud of dots.

3.2.2 Results

Figure 1d (conditions (a) and (b)) shows the results on these tasks from eight observers. Consistent with previously published literature, for all subjects the straight-line heading (Heading RDK) without objects was slightly easier than the Heading-RDK with objects, as reflected by the thresholds on the two tasks which referred to the judgment error between the true heading (FOE) and the probe.

3.2.3 Heading in the Presence of Landmarks

(c) The stimulus (shown schematically in Figure 1c) was a colored naturalistic display with texture mapped objects and complex 3-D structures portraying a large room with furniture, walls, and objects. The movement of the display simulated the direction of translation of an observer. The starting position was randomly generated from the central 2/3 of the room width and then the target of heading was chosen randomly at the right or left of the central fixation mark. The stimulus subtended 44×44 deg from a viewing distance of 30 cm. For each trial the first frame of the motion sequence portraying the room was displayed on the screen before the trial began. Observers were asked to fixate on a cross in the center of the display and watch the motion sequence for 1.9 seconds at the end of which the fixation mark disappeared. A vertical probe in the form of an hourglass was shown on a static view of the room and observers where asked to judge whether they were heading to the left or to the right of the probe via a button press. As in

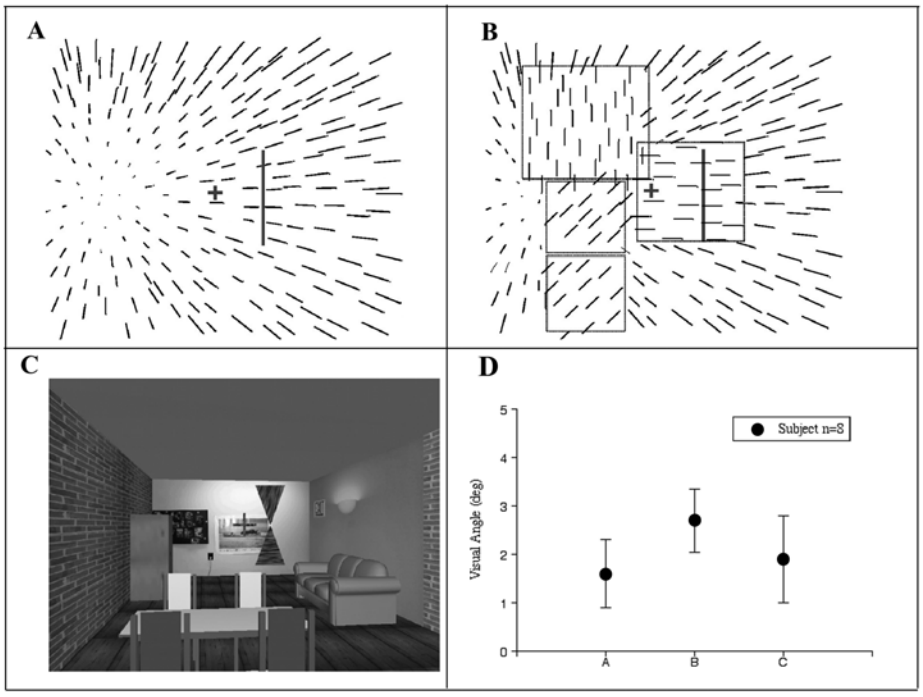

Figure 1. Heading stimuli and psychophysical performance of all subjects for each heading task. a) *Heading RDK*. b) *Heading RDK Objects*. c) *Heading Landmarks*. d) The mean final thresholds from all subjects reported for each heading task.

the previous heading task, an adaptive staircase was used to vary the angle between the true heading and the probe.

3.2.4 Results

Figure 1d (condition (c)) shows mean results from six staircases of eight observers. As before, the y-axis portrays the difference in degrees of visual angle between the true FOE and the probe. The difference among the results from the three tests was not statistically significant (t-test, $p>0.05$).

3.3 FMRI Data Acquisition and Experimental Design

Data were acquired in a 1.5-T whole-body MRI system (Magnetom Vision, Siemens, Germany) equipped with a head volume coil (with 40 mT/m

maximum gradient strength, a slew rate of 200 (T/m)/sec and a FOV of 40 cm). For fMRI, echo planer imaging (EPI), sensitive to blood oxygen level dependent (BOLD) effects, was used (repetition time TR = 2.53 sec, echo time TE = 70 ms, flip angle 90°, field of view 200 mm). To cover the whole brain, we used twenty two 5 mm thick slices with 1 mm gap with an axial orientation and an image size of 64×64 pixels. The slices covered the whole brain with a voxel size of 3.13×3.13×6 mm for the EPI images. For anatomical localization, we used 3-D gradient echo T1-weighted images (TR = 11.1 ms, TE = 4.3 ms, flip angle 8°, FOV 256 mm). Anatomical image size was 256×256×128 pixels, with a slice thickness of 1.33 mm, and voxel size of 1×1×1.33 mm. The stimuli were presented in a block design paradigm, alternating "fixation" as a baseline condition with one of the three stimuli, depending on the particular time series acquired. The subjects indicated their response by a button press on a magnet compatible keypad. The order of the tests was pseudo randomized and presentation was counterbalanced across subjects. The switching between the heading tasks was transmitted verbally. For every subject, each time series was repeated 3 times and for each of the eight subjects all data was obtained in a single scanning session.

Two additional time series were acquired from all subjects in which a passive viewing of a radially moving random dot kinematogram (10 deg in diameter, 6 deg/sec) embodied by white dots (6 arcmin in diameter) on a black background was interleaved with stationary dots of the same characteristics (except motion). A small white fixation mark was shown in the middle of the display and as previously, subjects were asked to maintain fixation. The motion alternated from trial to trial (1 sec each) between expansion and contraction. This condition was used for localizing the hMT+ complex in every subject.

3.4 FMRI data analysis

FMRI data were post processed using the MEDx 3.41 software package (Sensor Systems Inc., Sterling, VA) and complementary scripts (MEDx TCL, MATLAB (The Mathworks Inc., Natick, MA), and PERL) developed in our laboratory. Details of the initial steps of fMRI data analysis have been published (Vaina et al., 2001). Briefly, all individual functional images were motion-corrected (Woods, Grafton, Holmes et al., 1998; Woods, Grafton, Watson et al., 1998; Woods et al., 1993), spatially smoothed using a Gaussian filter (FWHM of two times the voxel size). Global intensity normalization was performed to normalize the average of each volume to the same mean value and linear signal intensity drift not related to the task under study was estimated for each voxel and removed from the time series data. Active brain

regions were determined by means of a t-test comparison of the rest and active conditions of each experimental paradigm and the timing of each paradigm condition were automatically recorded during each fMRI scan. The first four frames were removed from each acquisition to compensate for the effects of adaptation of a subject to the start of a new experimental run, and a five second delay was introduced into each paradigm file to account for the effects of hemodynamic delay in the fMRI responses. A statistical significance threshold of $P<0.05$ (Resel corrected) was applied to the data with an extent threshold of a minimum cluster size of four voxels (Worsley et al., 1992, 1996). For group analysis, statistical maps (z-values) for each subject in each condition were used to form a group statistical model by calculating the sum of individual z-values (over each voxel) divided by the square root of the number of subjects. For each subject, EPI images were registered to the high-resolution deskulled structural volume, the same transformation was applied to statistical volumes, registration in Talairach space (Talairach & Tournoux, 1988) was performed for the structural and statistical volumes, and thresholded statistical maps ($z \geq 3.0$ for individual subjects) were superimposed onto the high resolution structural volume.

A "goodness of data" test was performed to evaluate the similarity of statistical maps coming from the same paradigm acquisitions. The measure of similarity between statistical maps was based on the normalized cross-correlation commonly used in template matching. For a pair of statistical maps f and w the coefficient of normalized cross-correlation is given by

$$r = \frac{\sum_x \sum_y (f(x,y) - \overline{f})(w(x,y) - \overline{w})}{(\sum_x \sum_y (f(x,y) - \overline{f})^2 \sum_x \sum_y (w(x,y) - \overline{w})^2)^{1/2}} \quad (1)$$

summations are carried out over all pixels in the image. The measure of similarity defined above is based on the Schwartz inequality

$$\int fw \leq (\int f^2 \int w^2)^{1/2} \quad (2)$$

where f and w are two integrable, real-valued functions. It follows from the inequality that $-1 \leq r \leq 1$. Therefore, if statistical maps f and w coincide then $r = 1$, if they are not correlated $r = 0$, and if f and w are anti-correlated $r = -1$. After averaging the similarity measure over several slices, the result was compared to a threshold value set to 0.4. Data were considered to be good if similar acquisitions had the value of parameter r exceeding the threshold value set for the subject. Two weakly correlated acquisitions were found and

they were removed from further analysis. In one subject the data was inconsistent from one time series to another across every task and furthermore this subject had significant head movement. This subject was discarded from the further analysis of fMRI data.

To achieve a statistically sensitive analysis in a larger number of brain regions, we defined several regions of interests (ROIs) based on activations obtained in the initial statistical analysis of the data and previously reported results on brain areas involved in visual processing in humans, including tasks directly relevant to our study such as topographical navigation and judgment of heading (Aguirre & D'Esposito, 1997; Aguirre et al., 1998; D'Esposito et al., 1998; Dupont et al., 1994, 1997; Howard et al., 1996; Mendola et al., 1999; Peuskens et al., 2001; Sunaert et al., 1999; Tootell et al., 1997; Vaina et al., 2001; Van Oostende et al., 1997; Zeki et al., 2003). It is important to note that the estimated percent BOLD signal change values for each functionally defined cortical region were obtained on the basis of ROIs defined for each individual subject in a group and not on the basis of the average statistical activation map obtained in the group analysis for an fMRI task. This approach is somewhat more complex than the group analysis frequently seen in the fMRI literature, but it has a net advantage in that it is significantly less prone to inter-subject variability in the Talairach space of brain areas with similar functional properties.

For each ROI defined from our own fMRI data we calculated the Talairach coordinates of its center, mean and standard deviation of fMRI signal percent change, activation volume (total number of voxels having $z \geq 3.0$), and asymmetry index (AI) (Binder et al., 1996; Desmond et al., 1995; Thulborn et al., 1999). To reduce the contribution of voxels exhibiting sustained negative BOLD responses associated with reductions in blood flow and neuronal activity (Shmuel et al., 2002), only voxels in which BOLD signal percent change was positive were included in calculation of the mean percent change and standard deviation. For each ROI, we estimated the variation of the mean percent change $P = \mu \pm \Delta\mu$ by the following formula

$$\Delta\mu \approx P_{\max} + \frac{S_p}{S}(\sigma - P_{\max}) \tag{3}$$

where $P_{\max}$ is a maximal percent change with the ROI, S_p is the area of the ROI adjusted to contain only voxels with positive signal percent change, and S is the area of the original ROI. For each experimental condition, bar plots of mean fMRI signal percent change together with error bars (of estimated variation) were plotted by ROIs. Furthermore, for each ROI we performed a three-way ANOVA to compare mean values of fMRI signal percent change with respect to the three factors: different tasks, subjects, and hemispheric

sides (Hogg & Ledolter, 1987), and a multiple comparison test (using Bonferroni adjustment) of means of fMRI signal percent change was used to determine in which task the fMRI response change was significantly different from that in other tasks (Hochberg & Tamhane, 1987).

To study the relationship of fMRI activation to the subject's psychophysical performance, we performed an analysis of the correlations between fMRI responses and behavioral data. For all subjects (n=7) scatter plots showing normalized fMRI activation vs. normalized psychophysical performance for the individual subjects and specific tasks were generated for each ROI (Gilaie-Dotan et al., 2001) – the high correlation value ($r > 0.4$) indicates involvement of an ROI in processing of the visual task.

3.4.1 Results

The data from seven subjects was analyzed following all stages described above. First, statistical analysis of the fMRI data was conducted to determine the brain regions that may be involved in some or all three heading tasks used in this study. Group activation maps for the seven subjects on the three heading tasks are shown in axial brain slices registered in the Talairach space (Figure 2). By and large, the activation maps were similar for all heading tasks. The activated voxels in the occipital lobe were located in the fusiform gyrus (BA 17, 18), the cuneus (BA 18) and middle occipital gyrus (BA 18, 19). Activated voxels in the temporal lobe having z-values below threshold value of 5.7 (not visible in Figure 2), were located in the superior temporal gyrus (BA 22), middle and superior temporal gyrus, (BA 21, 22). Activated voxels in the parietal lobe (not shown) were located in inferior parietal lobule (BA 40), precuneus and superior parietal lobule (BA 7). The main focus of activation in the frontal lobe was located in precentral gyrus (BA 6). For reference, the hMT+ complex was localized in each subject and the mean area of activation for the seven subjects is outlined with concentric circles.

A subsequent analysis at a finer scale of resolution was carried out in order to reveal any significant differences across tasks in the level of fMRI responses. We defined separately for each task and subject several ROIs as described in the Methods section. The average values (over the seven subjects) of Talairach coordinates of the ROIs defined, standard deviations, corresponding maximal Z values, and tentative functional names are shown in Table 1.

After labeling each ROI with a tentative functional name, we estimated BOLD percent signal change within the functional regions defined for each task and for every subject. The estimated signal change values were averaged over all the subjects (n=7, shown in Figure 3).

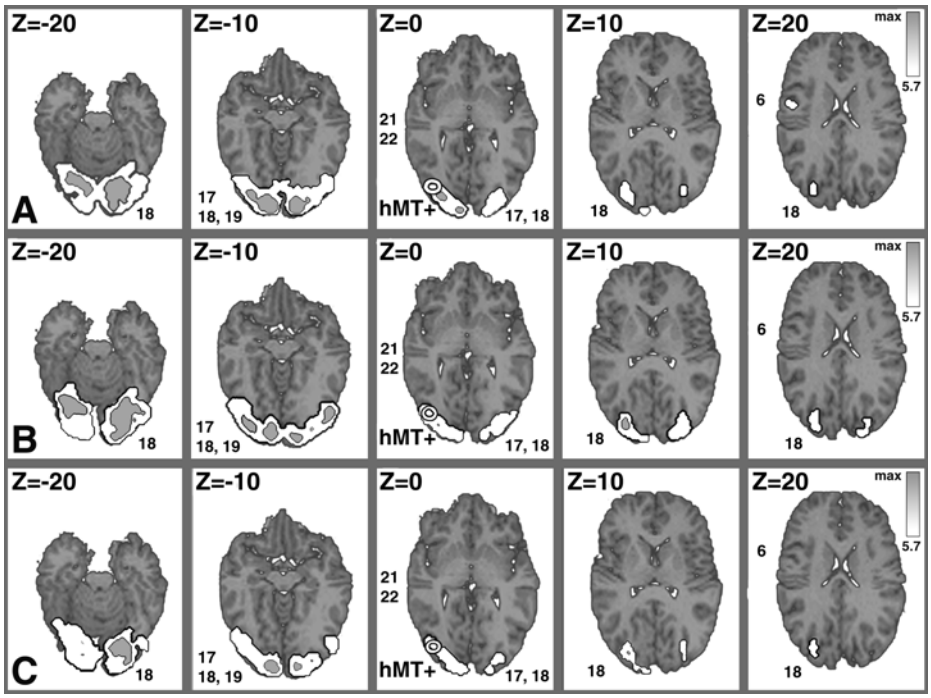

Figure 2. Activation regions for control subjects thresholded at z = 5.7 (n = 7). a) Averaged statistical map for the *Heading RDK* experiment. b) Averaged statistical map for the *Heading RDK Objects* experiment. c) Averaged statistical map for the *Heading Landmarks* experiment. Data was collected in a 1.5T scanner. Area hMT+ is outlined in a white circle.

To determine whether there were significant differences in activation levels within ROI's (Table 1) among the three tasks, subjects, and side of activity, we performed a three-way ANOVA and multiple comparisons analysis (see methods section). By and large the activations levels were similar across tasks and most ROI's. Significant differences were found only in V2 ($p = 1.7e\text{-}09$; $F = 62.68$) due to higher activation level in *Heading Landmarks* than in the other two tasks, V3a ($p = 5.93e\text{-}05$; $F = 21.11$) and KO/V3b ($p = 0.02$; $F = 5.49$) due to higher activation in the *Heading RDK-Objects* and *Heading Landmarks* than in *Heading RDK*, and PreCs ($p = 0.02$; $F = 9.64$,) due to higher activation level in *Heading RDK Objects* than in the other two tasks. As one would expect, these results illustrate that the more complex experimental situations portrayed by *Heading RDK-Objects* and *Heading Landmarks* stimuli were selectively associated with a higher signal change in several ROI's than the simpler *Heading RDK* task that simulates the flow field of an observer traveling on straight path in a rigid environment.

Table 1. For each ROI defined based on the initial statistical analysis of fMRI data for all heading tasks for several subjects (n=7) participated in the study, the table contains the ROI's tentative functional name, its stereotaxic coordinates (mean, std) and activation level (max Z value, std).

Stereotaxic coordinates and activation level for each ROI defined

ROI	Stereotaxic coordinates	Z values
V1	12.5 (0.9); -90.2 (2.5); -12.0 (0.0)	7.4 (2.9)
	-12.7 (1.8); -94.9 (1.3); -12.3 (0.7)	5.6 (3.4)
V2	29.4 (0.6); -84.5 (1.5); -11.0 (0.0)	6.1 (2.8)
	-26.6 (1.3); -86.8 (1.0); -11.0 (0.0)	5.6 (3.8)
VP	40.7 (3.3); -71.0 (1.7); -11.0 (0.0)	6.2 (3.3)
	-42.7 (1.8); -73.0 (2.3); -10.9 (0.4)	6.2 (2.6)
V3	15.7 (0.5); -93.9 (0.8); 7.3 (0.7)	4.7 (3.0)
	-18.0 (0.0); -92.7 (0.5); 7.0 (0.0)	3.9 (2.8)
V4	28.8 (5.2); -64.0 (4.2); -17.0 (0.0)	6.4 (3.1)
	-25.6 (3.7); -67.5 (1.4); -19.0 (0.0)	5.9 (3.8)
V3a	26.0 (0.3); -81.5 (1.9); 15.0 (0.0)	5.3 (3.8)
	-24.6 (1.4); -80.6 (3.0); 15.0 (0.0)	3.7 (2.0)
KO	28.2 (1.0); -84.7 (1.8); 2.0 (0.0)	5.4 (3.2)
	-27.6 (0.7); -84.2 (1.0); 2.0 (0.0)	4.4 (2.3)
MT	41.4 (3.1); -69.1 (1.3); -2.1 (0.4)	5.1 (2.5)
	-41.4 (2.4); -72.0 (2.9); -1.9 (0.8)	4.9 (2.1)
STS	54.6 (0.5); -37.3 (0.7); 5.0 (0.0)	1.3 (2.1)
	-53.3 (2.2); -39.5 (0.2); 5.5 (0.9)	1.4 (2.2)
STG	57.2 (0.2); -0.6 (1.4); 5.0 (0.0)	1.8 (2.3)
	-52.2 (1.8); -4 .0 (4.0); 5.5 (1.4)	1.4 (1.1)
PreCs	44.4 (2.1); -1.9 (3.6); 31.5 (3.0)	5.1 (2.5)
	-46.2 (1.3); -2.2 (2.4); 30.0 (0.0)	4.5 (3.2)
PostCs	28.8 (1.6); -51.4 (1.2); 37.3 (1.6)	4.9 (3.3)
	-32.2 (3.4); -49.3 (2.4); 36.1 (2.5)	4.7 (2.4)
DIPSM/L	13.4 (2.3); -72.9 (2.7); 41.8 (0.7)	6.7 (3.4)
	-16.9 (0.9); -71.9 (1.2); 42.0 (0.0)	7.3 (3.0)
SFS	23.0 (2.6); -13.3 (2.5); 52.3 (1.3)	5.0 (4.2)
	-26.0 (1.5); -15.5 (1.3); 50.5 (2.3)	4.1 (2.8)
PhG	26.6 (3.3); -48.0 (3.8); -20.0 (2.1)	3.2 (2.2)
	-29.2 (1.5); -51.3 (5.2); -19.9 (1.8)	2.9 (2.6)

3.5 Direct Correlation Between FMRI Signal and Performance on the Heading Tasks

We determined quantitatively the extent to which there was a direct correlation between the recorded fMRI signals and subjects' psychophysical performance measured by their responses during the fMRI scanning session. Figure 4 shows the relationship between normalized fMRI signal and subjects' normalized performance on the three tasks for several ROI's (Gilaie-Dotan et al., 2001). We considered the correlation to be significant if its correlation value (r) exceeded 0.4. For the *Heading RDK* task, the highest correlation between performance and normalized signal was in the functional area DISPM/L (r = 0.83) and a weaker correlation in the PostCS (r = 0.44) and VP (r = 0.41). This result strengthens Peusken's et al. (2001) suggestion that, compared with other parietal motion areas, the DISPM/L region of the posterior portion of the intraparietal sulcus is specifically tuned to heading estimation.

Behavioral responses in the *Heading RDK Objects* task were significantly correlated in area KO (r = 0.74), STS (r = 0.63), hMT+ (r = 0.53), V3 (r = 0.53) and V3a (r = 0.49), suggesting that the subjects might have computed, both motion and object borders when doing this heading task. Activity in both the PreCs (r = 0.76), and PostCs (r = 0.72) were also highly correlated with behavior. These areas are part of the frontoparietal network related to visual attention and oculomotor processing (Corbetta, 1998). Considering the three areas that were most correlated with behavior suggests that in order to compute heading direction in the presence of multiple moving objects, the visual system uses the relative motion system to segment and eliminate the objects. We suggest that the extraction of the kinetic objects occurs under the control of spatial attention (Corbetta, 1998; Vaina et al., 2001).

In the *Heading Landmarks* task the most significant correlations with behavior was found in STG (r = 0.64) followed by somewhat weaker correlations in V3 (r = 0.51), V3a (r = 0.69), and KO (r = 0.40). The Talairach coordinates of the center of area STG here, corresponds to a region suggested by previous functional neuroimaging studies (Howard et al., 1996, Vaina et al., 2001) as a human homologue of the macaque Superior Temporal Sulcus (Stp). It has been proposed that STP integrate motion information from the dorsal visual stream and object information from the ventral visual stream (Racine et al., 1996; Vaina & Gross, (submitted)). Both types of information coexist in this task and they might be used in concert to discriminate direction of heading in a scene populated with objects. Alternatively, object information may be extracted but not necessarily used in performing this task,

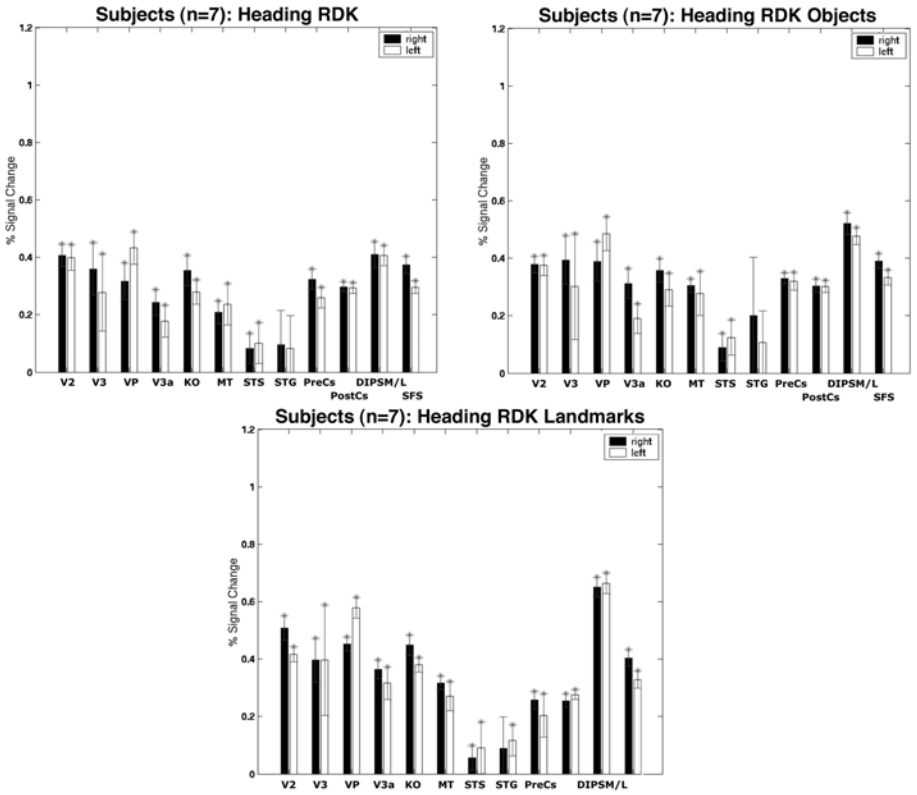

Figure 3. ROI analysis for control subjects (n=7). The bar graphs show the percent change in the fMRI signal within each ROI. Each pair of bars shows signal change in both the right and left hemispheres. Error bars indicate error estimates calculated as described in the methods section. Results from heading RDK (left), heading objects (right), and heading landmarks experiments (bottom) are shown.

since information from optic flow that is still present in the scene might be sufficient for judging the direction of heading.

The results of heading discrimination presented here are consistent with previous data on the same tasks from neurological patients with discrete lesions. For example, the suggestion of the important role in heading estimation of area DIPSM/L compared to other parietal areas ((Peuskens et al., 2001) and the data presented here), is strongly supported by our previous reports on neurological patients with bilateral posterior parietal lesions suffering of the Balint-Holmes syndrome, whose low level motion perception was normal, but perception of optic flow patterns, especially heading perception (Jornales et al., 1997; Vaina, 1998; Vaina & Rushton, 2000) was

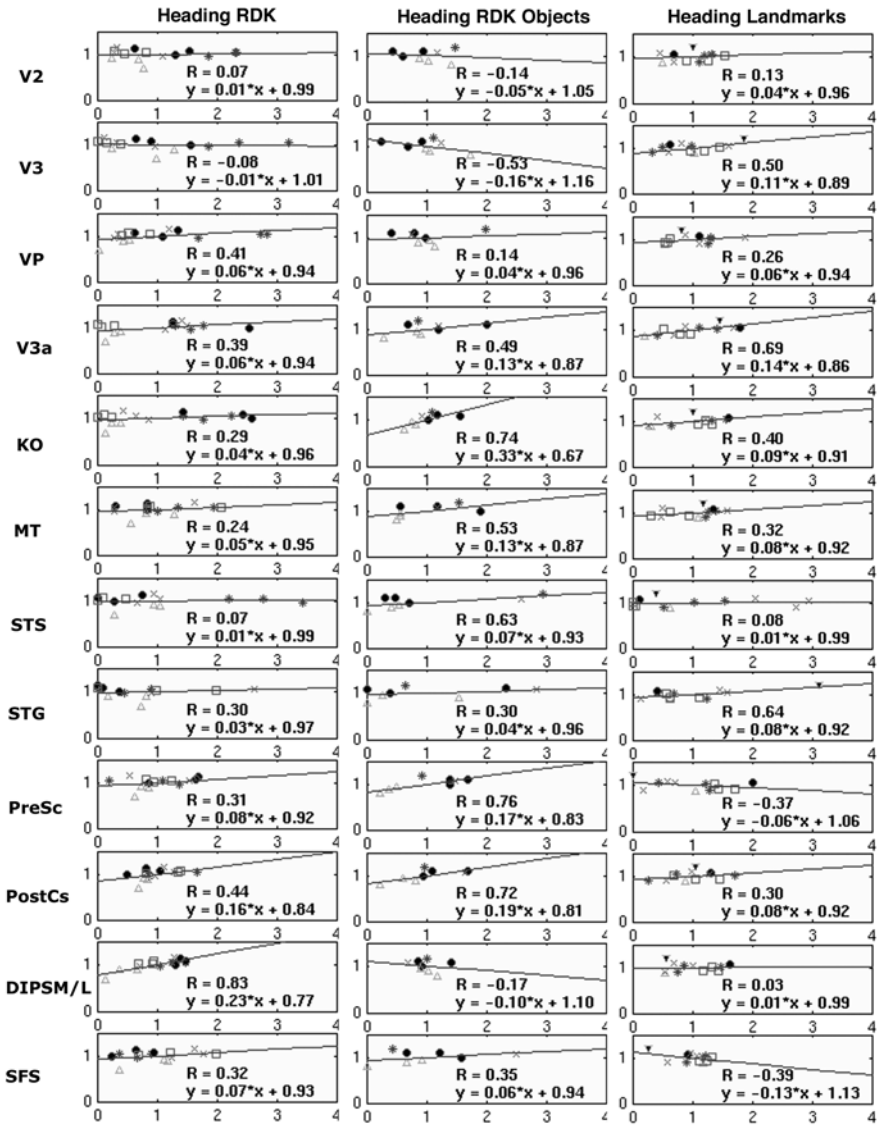

Figure 4. Correlation between subjects' behavioral performance and fMRI activation for the different ROIs. Scatter plots showing normalized fMRI activation (x-axis) vs. normalized recognition (y-axis) rate for the individual subjects (each subject is shown by different marker style) and specific heading tasks, *Heading RDK* (left column), *Heading RDK Objects* (middle column), and *Heading Landmarks* (right column). Results from each ROI are shown separately, in different rows. The regression line (solid), its equation and correlation value (R) are given for each plot.

severely impaired. These patients were first studied with the straight line *Heading RDK* stimulus that we also used in fMRI. Interestingly, while they remained unable to discriminate heading from random dot kinematograms, two of these patients had normal performance on the discrimination of *Heading Landmarks* task. (The third patient was not tested). Revisiting the specific brain areas correlated with behavior in the fMRI study described here, we note that they overlap very little, suggesting that different neuronal mechanisms may be used to judge direction of heading in the two tasks. Moreover, the areas significantly correlated with behavior in the *Heading Landmarks* task were not involved in these patients' lesions.

But still, how can the perception of self-motion occur without using optic flow? Several psychophysical studies showed (Cutting et al., 1992, 1997; Vaina & Rushton, 2000; Vishton & Cutting, 1995) that heading perception was possible even when instead of smooth motion observers view discrete samples, suggest that velocity information is not necessary for heading computation.

We explored this alternative by modifying the stimulus presentation in the *Heading Landmark* task (Figure 5). We removed the motion information by displaying three different static frames extracted from the motion of the room, each shown for 665 msec with interleaved blank intervals of 285 msec each. Five subjects, naïve to task and conditions were presented with this *Choppy Heading Landmarks* display (Figure 5b) and, as previously, were asked to determine whether their direction of heading was to the left or to the right of a probe. Figures 5c and d show psychophysical results for several subjects (n=5) and fMRI activation from a representative subject. As expected, subjects were unable to perceive heading in the sequence of static frames extracted from the heading RDK in which the only cue to calculate heading was provided by motion. In the Heading Landmark tasks, there was the motion cue but also the landmarks information. Eliminating motion information subjects presumably still could use the landmark cues to compute their heading. Figure 5d revealed a strong and stimulus specific activation of the parahippocampal gyrus in the *Choppy Heading Landmarks* condition.

This activation is consistent with results from a recent study by Gron and colleagues (Gron et al., 2000) that found when objects were used as specific landmarks for navigation during encoding of a maze there was a significant activation in the parahippocampal gyrus. Aguirre and D'Esposito (Aguirre & D'Esposito, 1997; Aguirre et al., 1998) also showed activity in the parahipocampal gyrus during subjects' acquisition of spatial layout for navigation. These results, taken together with our data from the *Choppy Heading Landmarks* suggest that when optic flow is not available for navigation, the computation of heading direction may be based on the knowledge of the spatial layout of the environment.

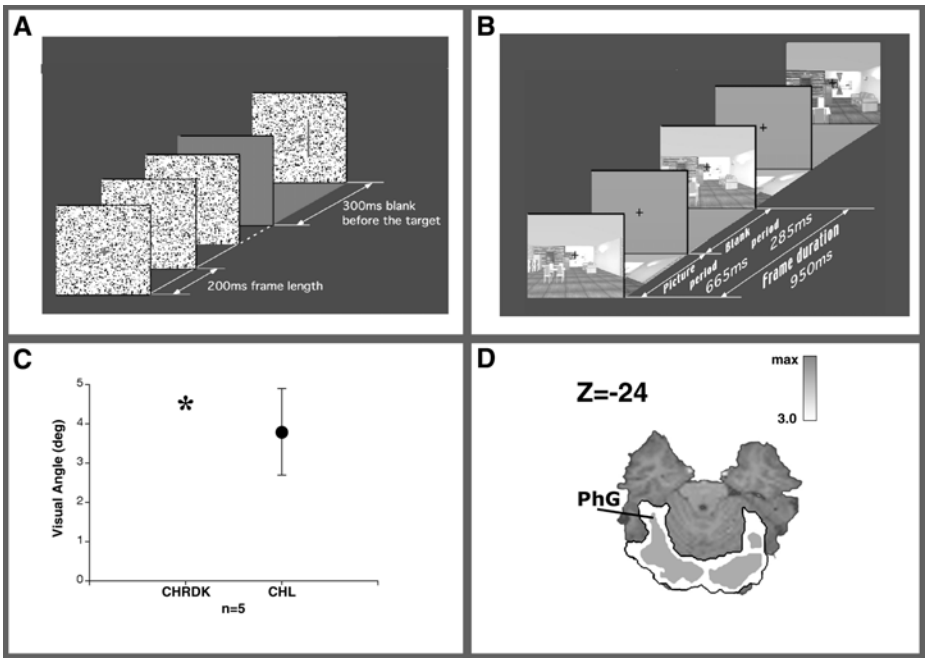

Figure 5. Choppy heading tests stimuli and results. a) Schematic view of the *Choppy Heading RDK* test. b) Schematic view of the *Choppy Heading Landmarks* test. In both *Choppy Heading RDK* and *Choppy Heading Landmarks* the probe was displayed in the last frame and subjects were asked to report whether they were heading to the left or right of the probe. c) Psychophysical data from five subjects on the *Choppy Heading RDK* (CHRDK) and *Choppy Heading Landmarks* (CHL) tasks. The asterisk denotes that subjects could not perform the task. The stimulus was presented with central fixation. d) Representative subject's brain slice indicating activity during presentation of the CHL test in the parahippocampal gyrus (PhG), an area that did not elicit activation by any other heading task described in this paper. (*Choppy Heading RDK* was not used in the fMRI).

4 WHERE ARE WE GOING?

Figure 6 is an illustrative summary of the major cortical regions we found activated by the three major heading tasks carried out in our laboratory, in relation with the functional neuroimaging studies of heading judgment briefly summarized at the beginning of the chapter. The different experimental paradigms, stimuli and imaging modalities used by the various studies might have contributed to the difference in results. However, all concur to support the view that judgment of heading direction engages a network of widely distributed neural regions which may be, at least in part, determined by the nature of the stimulus and the task.

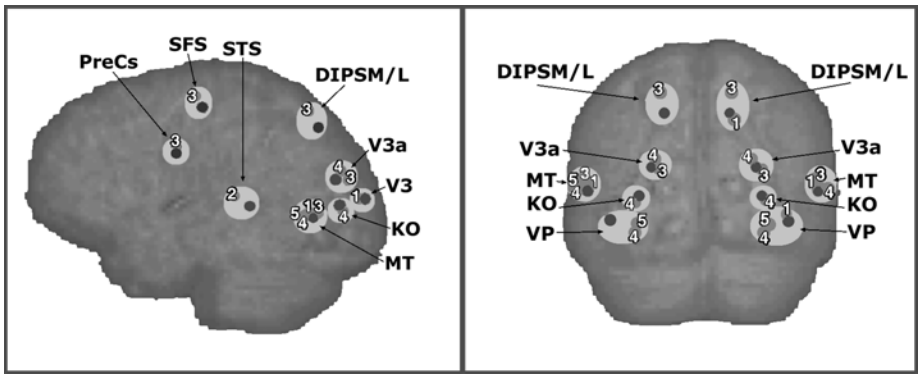

Figure 6. Location of brain areas involved in the visual heading estimation superimposed onto the brain of a typical normal subject. Lateral view of the left hemisphere (left) and posterior view of the back of the brain (right) is shown. Activations are shown in the Talairach coordinates (Talairach & Tournoux, 1988). Black disks show location of the activated areas according to the present study, dark gray disks show activated areas location according to 1 = (de Jong et al., 1994), 2 = (Howard et al., 1996), 3 = (Peuskens et al., 2001), 4 = (Rutschmann et al., 2000), 5 = (Wunderlich et al., 2002). Light gray disks summarize results of the present and previous studies into several clusters of areas corresponding to the following ROIs: VP, V3, V3a, KO, MT, STS, PreCs, DIPSM/L, STS.

In view of the ongoing controversies regarding the mechanisms involved in computing self- motion, and because of the importance of heading computation for locomotion and ultimately for action, further studies are needed to pin down the specific functional neuroanatomy of motion for navigation. The current psychophysical theories of self motion perception complemented by predictions from emerging computational models constrained by the newer results from monkey physiology, offer a great opportunity for well designed, hypothesis driven, functional neuroimaging studies of the possible underlying neural mechanisms of heading.

However, limiting the inquiry to just the perceptual investigation will not give us the full answer, because in the psychophysical tasks the human subjects are asked to indicate to which side of a reference mark they are heading, and it is an inference that their responses reflect a judgment of heading (Wurtz, 1998). But this is the best approximation of the problem we now have on our hands, before quantitative studies of heading estimation in subjects navigating in the real everyday environment emerge with some consistency. There are encouraging signs that this is already beginning to happen. Several laboratories are using head mounted displays and virtual reality to study heading and navigation in normal (Tarr & Warren, 2002) and neurological human subjects (Wann, 1996). Before long these displays will be MR compatible and we will be able to quantitatively measure what the brain

is doing when it navigates through a busy world, compare walking in a desert to walking in the busy New York City at rush hour, or to running on the most crooked street in San Francisco.

4.1 Acknowledgments

We thank Martin Kopcik for programming the psychophysical and fMRI stimuli used here. We thank Rosalyn Ano for help with the fMRI data analysis, and Winfred Kao for technical support in acquiring the fMRI data. This work was supported by a grant from the National Institutes of health, EY-2R01-07861-13 to LMV.

5 REFERENCES

Aguirre, G. K., & D'Esposito, M. (1997). Environmental knowledge is subserved by separable dorsal/ventral neural areas. *J. Neurosci., 17* (7), 2512-2518.

Aguirre, G. K., Zarahn, E., & D'Esposito, M. (1998). Neural components of topographical representation. *Proc. Natl. Acad. Sci. USA., 95* (3), 839-846.

Albright, T.D. (1993). Cortical processing of visual motion. In: F.A. Miles, & J. Wallman (Eds.), *Visual Motion and its Role in the Stabilization of Gaze* (pp. 177-201): Elsevier Science Publishers B.V.

Albright, T.D., & Stoner, G.R. (1995). Visual Motion Perception. *Proc. Natl. Acad. Sci. USA., 92*, 2433-2440.

Andersen, R.A. (1997). Neural mechanisms of visual motion perception in primates. *Neuron, 18*, 865-872.

Andersen, R. A., Shenoy, K. V., Crowell, J. A., & Bradley, D. C. (2000). Neural Mechanisms for Self-Motion Perception in Area MST. In: M. Lappe (Ed.) *Neuronal Processing of Optic Flow,* 44 (pp. 219-233). New York: Academic Press.

Beauchamp, M., & DeYoe, E. (1996). Brain areas for processing motion and their modulation by selective attention. *NeuroImage, 3*, 245.

Beer, J., Blakemore, C., Previc, F. H., & Liotti, M. (2002). Areas of the human brain activated by ambient visual motion, indicating three kinds of self-movement. *Exp. Brain Res., 143* (1), 78-88.

Binder, J. R., Swanson, S .J., Hammeke, T. A., Morris, G. L., Mueller, W. M., Fischer, M., Benbadis, S., Frost, J. A., Rao, S. M., & Haughton, V. M. (1996). Determination of language dominance using functional MRI: a comparison with the Wada test. *Neurology, 46* (4), 978-984.

Braddick, O. J., O'Brien, J. M., Wattam Bell, J., Atkinson, J., Hartley, T., & Turner, R. (2001). Brain areas sensitive to coherent visual motion. *Perception, 30* (1), 61-72.

Britten, K. H., & Van Wezel, R. J. (1998). Electrical microstimulation of cortical area MST biases heading perception in monkeys. *Nat. Neurosci., 1* (1), 59-63.

Britten, K. H., & Van Wezel, R. J. (2002). Area MST and heading perception in macaque monkeys. *Cereb. Cortex, 12* (7), 692-701.

Cheng, K., Fujita, H., Kanno, I., Mura, S., & Tanaka, K. (1995). Human Cortical Regions Activations by Wide Field Visual Motion: An H2(15)O PET Study. *J. Neurophysiol., 74* (1), 413-426.

Corbetta, M. (1998). Frontoparietal cortical networks for directing attention and the eye to visual locations: Identical, independent, or overlapping neural systems? *Proc. Natl. Acad. Sci. USA, 95* (3), 831-838.

Cutting, J. E., Springer, K., Braren, P. A., & Johnson, S. H. (1992). Wayfinding on foot from information in retinal, not optical, flow. *J. Exp. Psychol. Gen., 121* (1), 41-72.

Cutting, J. E., Vishton, P. M., Fluckiger, M., Baumberger, B., & Gerndt, J. D. (1997). Heading and path information from retinal flow in naturalistic environments. *Percept. Psychophys., 59* (3), 426-441.

D'Avossa, G., & Kersten, D. (1996). Evidence in human subjects for independent coding of azimuth and elevation for direction of heading from optic flow. *Vision Res., 36* (18), 2915-2924.

D'Avossa, G., Yacoub, E., Kersten, D., & Hu, X. (1998). Optic flow simulating eccentric ego-motion cause "activation" in occipito parietal areas of the contralateral hemisphere. *Invest. Opthalmol. Vis. Sci., 39* (4), 467.

D'Esposito, M., Aguirre, G. K., Zarahn, E., Ballard, D., Shin, R.K., & Lease, J. (1998). Functional MRI studies of spatial and nonspatial working memory. *Cogn. Brain Res., 7* (1), 1-13.

de Jong, B. M., Shipp, S., Skidmore, B., Frackowiak, R. S., & Zeki, S. (1994). The cerebral activity related to the visual perception of forward motion in depth. *Brain, 117*, 1039-1054.

Desmond, J. E., Sum, J. M., Wagner, A. D., Demb, J. B., Shear, P. K., Glover, G. H., Gabrieli, J. D., & Morrell, M. J. (1995). Functional MRI measurment of language lateralization in Wada-tested patients. *Brain, 118* (6), 1411-1419.

Dukelow, S. P., DeSouza, J. F., Culham, J. C., Van Den Berg, A. V., Menon, R. S., & Vilis, T. (2001). Distinguishing subregions of the human MT+ complex using visual fields and pursuit eye movements. *J. Neurophysiol., 86*, 1991-2000.

Dumoulin, S. O., Baker, C. L., Hess, R. F., & Evans, A. C. (2003). Cortical specialization for processing first- and second-order motion. *Cereb. Cortex, 13* (12), 1375-1385.

Dupont, P., De Bruyn, B., Vandenberghe, R., Rosier, A., Michiels, J., Marchal, G., Mortelmans, L., & Orban, G.A. (1997). The kinetic occipital region in human visual cortex. *Cereb. Cortex, 7*, 283-292.

Dupont, P., Orban, G. A., De Bruyn, B., Verbruggen, A., & Mortelmans, L. (1994). Many areas of the human brain respond to visual motion. *J. Neurophysiol., 72* (3), 1420-1424.

Gibson, J. J. (1950). *The perception of the visual world*. Boston: Houghton Mifflin.

Gilaie-Dotan, S., Ullman, S., Kushnir, T., & Malach, R. (2001). Shape-selective stereo processing in human object-related visual areas. *Hum. Brain Mapp., 15*, 67-79.

Greenlee, M. W. (2000). Human Cortical areas underlying the perception of optic flow: brain imaging studies. *Int. Rev. Neurobiol., 44*, 269-292.

Grezes, J., Fonlupt, P., Bertenthal, B., Delon-Martin, C., Segebarth, C., & Decety, J. (2001). Does perception of biological motion rely on specific brain regions? *NeuroImage, 13*, 775-785.

Gron, G., Wunderlich, A. P., Spitzer, M., Tomczak, R., & Riepe, M. W. (2000). Brain activation during human navigation: gender-different neural networks as substrate of performance. *Nat. Neurosci., 3* (4), 404-408.

Grossman, E., Donnelly, M., Price, R., Pickens, D., Morgan, V., Neighbor, G., & Blake, R. (2000). Brain Areas Involved in Perception of Biological Motion. *J. Cogn. Neurosci., 12* (5), 711-720.

Grossman, E. D., & Blake, R. (2002). Brain Areas Active during Visual Perception of Biological Motion. *Neuron, 35* (6), 1167-1175.

Hochberg, Y., & Tamhane, A. (1987). Multiple Comparison Procedures. New York: Wiley.

Hogg, R. V., & Ledolter, J. (1987). Engineering Statistics. MacMilan Publishing Company.

Howard, R. J., Brammer, M., Wright, I., Woodruff, P. W., Bullmore, E. T., & Zeki, S. (1996). A direct demonstration of functional specialization within motion-related visual and auditory cortex of the human brain. *Curr. Biol., 6* (8), 1015-1019.

Huk, A. C., Dougherty, R. F., & Heeger, D. J. (2002). Retinotopy and functional subdivision of human areas MT and MST. *J. Neurosci., 22* (16), 7195-7205.

Jornales, V. E., Jakob, M., Zamani, A., & Vaina, L. M. (1997). Deficits on complex motion perception, spatial discrimination, and eye-movements in a patient with bilateral occipital-parietal lesions [ARVO Abstract]. *Invest. Ophthalomol. Vis. Sci., 38* (4), S72.

Knudsen, E. I., DuLac, S., & Esterly, S. (1987). Computational maps in the brain. *Annu. Rev. Neurosci., 10*, 41-65.

McKeefry, D. J., Watson, J. D. G., Frackowiak, R. S. J., Fong, K., & Zeki, S. (1997). The activity in human areas V1/V2, V3, and V5 during the perception of coherent and incoherent motion. *NeuroImage, 5* (1), 1-12.

Mendola, J., Dale, A., Fischl, B., Liu, A., & Tootell, R. (1999). The representation of illusory and real contours in human cortical visual areas revealed by functional magnetic resonance imaging. *J. Neurosci., 19* (19), 8560-8572.

Morrone, M. C., Tosetti, M., Montanaro, D., Fiorentini, A., Cioni, G., & Burr, D. C. (2000). A cortical area that responds specifically to optic flow, revealed by fMRI. *Nat. Neurosci., 3* (12), 1322-1328.

Orban, G. A. (2001). Neural coding in area MT/V5 and satellites: from antagonistic surround to the extraction of 3D structure from motion. In: W. Backhaus (Ed.) *Neural Coding of Perceptual Systems,* 9 (pp. 188-202). London: World Scientific Publishing Company.

Peuskens, H., Sunaert, S., Dupont, P., Van Hecks, P., & Orban, G. A. (2001). Human brain regions involved in heading estimation. *J. Neurosci., 21* (7), 2451-2461.

Racine, C., Vaina, L. M., Diaz, J., Zamani, A., & Gross, C. G. (1996). Are there specific anatomical correlates of biological perception in the human visual system? *Society for Neuroscience 26th Annual Meeting. Abstracts, 22* (1), 400.

Reppas, J. B., Niyogi, S., Dale, A. M., Sereno, M. I., & Tootell, R. B. (1997). Representation of motion boundaries in retinotopic human visual cortical areas. *Nature, 388* (6638), 175-179.

Royden, C. S., & Hildreth, E. C. (1996). Human heading judgments in the presence of moving objects. *Percept. Psychophys., 58* (6), 836-856.

Rutschmann, R., Schrauf, M., & Greenlee, M. W. (2000). Brain activation during dichoptic presentation of optic flow stimuli. *Exp. Brain Res., 134* (4), 533-537.

Servos, P., Osu, R., Santi, A., & Kawato, M. (2002). The neural substrates of biological motion perception: an fMRI study. *Cereb. Cortex, 12*, 772-782.

Shmuel, A., Yacoub, E., Pfeuffer, J., Van de Moortele, P., Adriany, G., Hu, X., & Ugurbil, K. (2002). Sustained negative BOLD, blood flow and oxygen consumption response and its coupling to the positive response in the human brain. *Neuron, 36*, 1195-1210.

Siegel, R. M. (1998). Representation of visual space in area 7a neurons using the cetner of mass equation. *J. Comput. Neurosci., 5* (4), 365-381.

Siegel, R.M., & Read, H.L. (1997). Analysis of optic flow in the monkey parietal area 7a. *Cerebral Cortex, 7* (4), 327-346.

Smith, A. T., Greenlee, M. W., Singh, K. D., Kraemer, F. M., & Hennig, J. (1998). The processing of first- and second-order motion in human visual cortex assessed by functional magnetic resonance imaging (fMRI). *J. Neurosci., 18*, 3816-3830.

Sunaert, S. (2001). Functional magnetic resonance imaging: Studies of visual motion processing in the human brain. *ACTA Biomedica Lovaniensia, 226*, 1-123.

Sunaert, S., Van Hecke, P., Marchal, G., & Orban, G. A. (1999). Motion-responsive regions of the human brain. *Exp. Brain Res., 127* (4), 355-370.

Sunaert, S., Van Hecke, P., Marchal, G., & Orban, G. A. (2000). Attention to speed of motion, speed discrimination, and task difficulty: An fMRI study. *NeuroImage, 11* (6), 612-623.

Talairach, J., & Tournoux, P. (1988). Co-Planar Stereotaxic Atlas of the Human Brain. New York: Thieme Medical Publishers.

Tarr, M. J., & Warren, W. H. (2002). Virtual reality in behavioral neuroscience and beyond. *Nat. Neurosci., 5 (Supplement)*, 1089-1092.

Thulborn, K. R., Carpenter, P. A., & Just, M. A. (1999). Plasticity of language-related brain function during recovery from stroke. *Stroke, 30*, 749-754.

Tootell, R. B. H., Mendola, J. D., Hadjikhani, N. K., Ledden, P. J., Liu, A. K., Reppas, J. B., Sereno, M. I., & Dale, A. M. (1997). Functional analysis of V3a and related areas in human visual cortex. *J. Neurosci., 17* (18), 7060-7078.

Tootell, R. B. H., Mendola, J. D., Hadjikhani, N. K., Liu, A. K., & Dale, A. M. (1998). The representation of the ipsilateral visual field in human cerebral cortex. *Proc. Natl. Acad. Sci. USA, 95* (3), 818-824.

Tootell, R. B. H., Kwong, K. K., Belliveau, J. W., Baker, J. R., Stern, C. E., Hockfield, S. J., Breiter, H. C., Born, R., Benson, R., Brady, T. J., & Rosen, B. R. (1993). Mapping human visual cortex: evidence from functional MRI and histology. *Invest. Opthalmol. Vis. Sci., 34* (4), 813.

Tootell, R. B. H., Reppas, J. B., Dale, A. M., Look, R. B., Sereno, M. I., Malach, R., Brady, T. J., & Rosen, B. R. (1995a). Visual motion aftereffect in human cortical area MT revealed by functional magnetic resonance imaging. *Nature, 375*, 139-141.

Tootell, R. B. H., Reppas, J. B., Kwong, K. K., Malach, R., Born, R. T., Brady, T. J., Rosen, B. R., & Belliveau, J. W. (1995b). Functional analysis of human MT and related visual cortical areas using magnetic resonance imaging. *J. Neurosci., 15* (4), 3215-3230.

Vaina, L. M. (1998). Complex motion perception and its deficits. *Curr. Opin. Neurobiol., 8* (4), 494-502.

Vaina, L. M., & Gross, C. G. ((submitted)). Perceptual deficits in patients with impaired recognition of biological motion after temporal lesions.

Vaina, L. M., & Rushton, S. K. (2000). What neurological patients tell us about the use of optic flow. *Int. Rev. Neurobiol., 44*, 293-313.

Vaina, L. M., Solomon, J., Chowdhury, S., Sinha, P., & Belliveau, J. W. (2001). Functional neuroanatomy of biological motion perception in humans. *Proc. Natl. Acad. Sci. USA, 98* (20), 11656-11661.

Van Oostende, S., Sunaert, S., Van Hecke, P., Marchal, G., & Orban, G. A. (1997). The kinetic occipital (KO) region in man: an fMRI study. *Cereb. Cortex, 7*, 690-701.

Vishton, P. M., & Cutting, J. E. (1995). Wayfinding, displacements, and mental maps: Velocity fields are not typically used to determine one's heading. *J. Exp. Psychol. Hum. Percept. Perform., 21*, 978-995.

Wann, J. P. (1996). Virtual reality environments for rehabilitation of perceptual-motor disorders following stroke. *The First European Conference on Disability, Virtual Reality and Associated Technologies* (pp. 233-238). Maidenhead, U.K.

Warren, W. H. (1998). The state of flow. In: T. Watanabe (Ed.) *High-level motion processing* (pp. 315-358). Cambridge, MA: MIT Press.

Warren, W. H. (1999). Visually controlled locomotion, 40 years later. *Ecol. Psychol., 10* (3-4), 177-219.

Warren, W. H., & Saunders, J. A. (1995). Perceiving heading in the presence of moving objects. *Perception, 24* (3), 315-331.

Watson, J. D., Myers, R., Frackowiak, R. S., Hajnal, J. V., Woods, R. P., Mazziotta, J. C., Shipp, S., & Zeki, S. (1993). Area V5 of the human brain: evidence from a combined study using positron emission tomography and magnetic resonance imaging. *Cereb. Cortex, 3* (2), 79-94.

Woods, R. P., Grafton, S. T., Holmes, C. J., Cherry, S. R., & Mazziotta, J. C. (1998). Automated image registration: I. General methods and intrasubject, intramodality validation. *J. Comput. Assist. Tomogr., 22* (1), 139-152.

Woods, R. P., Grafton, S. T., Watson, J. D., Sicotte, N. L., & Mazziotta, J. C. (1998). Automated image registration: II. Intersubject validation of linear and nonlinear models. *J. Comput. Assist. Tomogr., 22* (1), 153-165.

Woods, R. P., Mazziotta, J. C., & Cherry, S. R. (1993). MRI-PET registration with automated algorithm. *J. Comput. Assist. Tomogr., 17* (4), 536-546.

Worsley, K. J., Evans, A. C., Marrett, S., & Neelin, P. (1992). A three-dimensional statistical analysis for CBF activation studies in human brain. *J. Cereb. Blood Flow Metab., 12* (6), 900-918.

Worsley, K. J., Marrett, S., Neelin, P., Vandal, A. C., Friston, K. J., & Evans, A. C. (1996). A unified ststistical approach for determining significant signals in images of cerebral activation. *Hum. Brain Mapp., 4*, 58-73.

Wunderlich, G., Marshall, J. C., Amunts, K., Weiss, P. H., Mohlberg, H., Zafiris, O., Zilles, K., & Fink, G. R. (2002). The importance of seeing it coming: a functional magnetic resonance imaging study of motion-in-depth towards the human observer. *Neuroscience, 112* (3), 535-540.

Wurtz, R. H. (1998). Optic flow: A brain region devoted to optic flow analysis? *Curr. Biol., 8* (16), 554-556.

Wurtz, R. H., & Duffy, C. J. (1992). Neuronal correlates of optic flow stimulation. *Ann. N. Y. Acad. Sci., 656*, 205-219.

Zeki, S., Perry, R. J., & Barteis, A. (2003). The processing of kinetic contours in the brain. *Cereb. Cortex, 2003* (13), 189-202.

Zeki, S., Watson, J. D. G., Lueck, C. J., Friston, K. J., Kennard, C., & Frackowiak, R. S. J. (1991). A direct demonstration of functional specialization in human visual cortex. *J. Neurosci., 11(3)*, 641-649.